Краткие сообщения ОИЯИ №2[65]-94 *JINR Rapid Communications No.2[65]-94*
УДК 539.143.43 + 539.143.5

Q-METER THEORY

Yu.F.Kisselev[1], C.M.Dulya[2], T.O.Niinikoski[3]

This paper develops the theory of series Q-meters used for measurements of NMR signals. For the first time we have derived closed form expressions for the nuclear susceptibility in terms of the Q-meter output voltage and for the residual Q-curve. We discuss the corrections involved in measuring nuclear polarization from NMR signals by using signals for the deuteron and proton as examples. Deuteron signals are shown to contain a false asymmetry, while proton signals have substantial distortions due to the long signal wings and the depth of modulation. Moreover, for the first time the importance of making a phase correction is demonstrated. We conclude that the series Q-meter with real part detection is not sufficient to produce an output voltage from which the nuclear susceptibility can be determined and thus an additional phase-sensitive detector is necessary for obtaining the imaginary part of the signal as well.

The investigation has been performed at CERN, Geneva.

Теория Q-метра

Ю.Ф.Киселев, К.М.Дулиа, Т.О.Ниииникоски

В работе осуществлено дальнейшее развитие теории последовательного Q-метра, прибора для измерения ядерной поляризации мишеней. Впервые получено выражение для ядерной восприимчивости мишени через выходное напряжение Q-метра. Обсуждается коррекция NMR протонных и дейтронных сигналов, используемых при измерении поляризации. Показано, что дейтронные сигналы содержат ложную асимметрию. Протонные сигналы существенно искажены дисперсионной компонентой при большой глубине модуляции. Демонстрируется важность нового типа фазовой коррекции. Анализ показывает, что последовательный Q-метр с детектором реальной компоненты сигнала не позволяет восстановить ядерную восприимчивость. Чтобы решить эту проблему, требуется дополнительный фазовый детектор мнимой компоненты сигнала.

Работа выполнена в ЦЕРН, Женева.

1. Introduction

The series Q-meter has found wide acceptance for the measurement of NMR spectra, especially in the precise measurement of nuclear polarization in polarized targets used in scattering experiments. Theoretical treatments

[1]Permanent address: Laboratory of Particle Physics, Joint Institute for Nuclear Research, Dubna, Moscow Region, Russia
[2]University of California, Department of Physics, Los Angeles CA 90024, USA
[3]CERN, CH-1211 Geneva 23, Switzerland

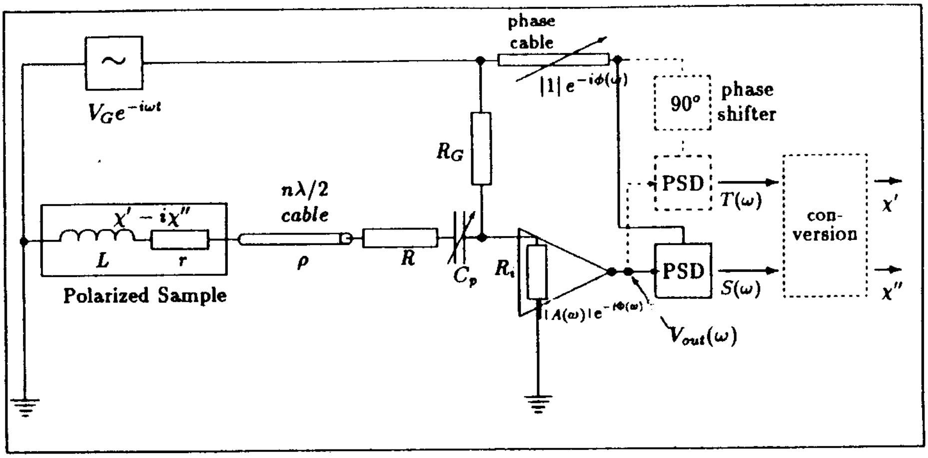

Fig.1. This is a block diagram of the Q-meter circuit detecting the real part of the NMR signal. The dashed lines correspond to the additions necessary to correct the Q-meter output signal such that the new outputs become proportional to the nuclear polarization

[1,2,3] have, until now, centered on approximate solutions of the equations for the Q-meter output voltage based on expansions in terms of the nuclear susceptibility using circuit elements as parameters. In this paper, we express the susceptibility as a function of the circuit parameters and the Q-meter output voltage and, furthermore, demonstrate general properties of the relationship between the Q-meter output signal and the susceptibility.

The sensing probe of the Q-meter circuit, shown on Fig.1, is a coil embedded in the material under study which couples inductively with the magnetic moments of the nuclei in that material. As a result of this interaction, the coil impedance Z_L varies linearly with the complex magnetic susceptibility $\chi(\omega)$ of the material according to[1]

$$Z_L = r + i\omega L(1 + \eta\chi(\omega)), \tag{1}$$

where $\omega = 2\pi\nu$, ν is the frequency of the rf generator, η is the effective filling factor of the material in the coil and L is the inductance of the NMR coil when $\chi = 0$. The complex function $\chi(\omega) = \chi'(\omega) - \iota\chi''(\omega)$ is the nuclear susceptibility of the material; its real part is called dispersion; and the imaginary part, absorption. The susceptibility is finite for all frequencies, but the dispersion changes the sign; it tends to have larger values in the vicinity of the Larmor frequency. The absorption describes the spectral distribution

[1]In MKSA units

of spins near the NMR Larmor frequency and its integral is proportional to the nuclear polarization. The constant of proportionality may be found by measuring the signal for samples in thermal equilibrium (TE) in a known magnetic field and temperature. In this case, the polarization is calculable from the Maxwell — Boltzmann distribution and is described by the Brillouin function.

In the Q-meter, the coil is usually connected to a room-temperature tuning capacitor and amplifier by a coaxial transmission line whose length is adjusted to an integer number of half-wavelengths at the Larmor frequency. These form a hybrid series tuned circuit [1]. Given the electrical parameters of the receiver circuitry and a well-defined NMR line shape, it is not difficult to calculate the Q-meter output voltage. In practice, however, we wish to solve exactly the opposite problem; namely to evaluate the complex magnetic susceptibility from the Q-meter signal. In this paper, we will review the theory of the Q-meter and apply these ideas to specific examples for proton and deuteron signals.

2. The Q-Meter Circuit

Since we are mainly concerned with series Q-meters using rf phase sensitive signal detection and homodyne receiver circuitry [4,5] as in Fig.1, we will incorporate the following definitions and values for the circuit parameters now:

Table of Circuit Parameters

Parameter	Description of parameter	Units	Typical value	
			Proton	Deuteron
ν_0	Larmor frequency	[MHz]	106.5	16.35
$\Delta\nu$	Range of frequency sweep	[kHz]	600	500
R_G	Feed resistance	[Ω]	900	900
R	Damping resistance	[Ω]	33	9
R_i	Amplifier input impedance	[Ω]	120	50
r	Coil resistance	[Ω]	0.3	0.3
C_p	Tuning capacitance	[pF]	19	200
L	Coil inductance	[μH]	0.091	0.48
ρ	Cable impedance	[Ω]	50	50
ε	Cable dielectric constant		2	2
α	Cable attenuation constant	[Np/m]	0.02	0.005
β	Cable phase constant $\beta = \omega\sqrt{\varepsilon}/c$	[m^{-1}]		

Para-meter	Description of parameter	Units	Typical value	
			Proton	Deuteron
l	Cable length $l = nc/2\nu_0\sqrt{\varepsilon}$	[m]	4.99	6.42
n	Number of cable half wavelengths		5	1
c	Speed of light	[m/s]	$2.9979 \cdot 10^8$	$2.9979 \cdot 10^8$
V_G	Voltage of high frequency synthesizer	[V]	0.1	0.1
$A(\omega)$	Gain of high frequency amplifier		50	50

The ouptput of the amplifier is connected to the input of a phase sensitive detector (PSD). The PSD selects the real part of the voltage at its input terminal relative to a reference voltage. This is the main idea of the Liverpool Q-meter [5]. In our conclusions, we will suggest the improvement of this Q-meter design by adding another PSD for selecting the imaginary part of the signal as well as the real part. Moreover, we also suggest a function that will transform the output voltage to be proportional to the complex nuclear susceptibility.

3. Determination of the Nuclear Susceptibility from the Q-Meter Signal

The nuclear polarization is proportional to the integral of the absorption, where the limits of integration are usually restricted to frequencies near the Larmor frequency (see Section 6). In other words, the polarization is given by

$$P = C \int_{\omega_{min}}^{\omega_{max}} \chi''(\omega) d\omega, \tag{2}$$

where C is a constant determined from calibration at TE. To calculate the polarization we thus need to know the absorption spectrum. Thus, one would like to write an equation for the susceptibility as a function of the Q-meter output voltage.

The Q-meter output voltage, which is the complex voltage at the output of the rf amplifier, is a function of the nuclear susceptibility. However, the effective filling factor of the coil, η, from Eq.(1) disappears for relative values of the polarization. Thus, we will define and calculate a complex function $\xi(\omega) = \eta\chi(\omega)$. The general expressions for the Q-meter output voltage [1,3] can be written in complex form [6] as

$$V_{out}(\omega) = \frac{V_n}{R_G} \frac{Z(\xi)}{1 + pZ(\xi)}, \tag{3}$$

where $Z(\xi)$ is the resonant circuit impedance

$$Z(\xi) = R - \frac{\iota}{\omega C_p} + \frac{\rho^2 \tanh(\gamma l) + \rho\,[r + \iota\omega L(1 + \xi)]}{\rho + [r + \iota\omega L(1 + \xi)] \tanh(\gamma l)}, \tag{4}$$

with

$$p = \frac{1}{R_i} + \frac{1}{R_G}, \qquad V_n = A(\omega) V_G \quad \text{and} \quad \gamma = \alpha + \iota\beta, \tag{5}$$

where γ is the complex propagation constant of the coaxial transmission line and α is its average attenuation constant. The coefficient p is the admittance due to the feed and the shunt resistances R_G and R_i. Table 1 describes the circuit parameters and gives their numerical values used in our estimations.

If the generator frequency is swept slowly enough so that $\xi(\omega)$ has no explicit time dependence, then the normalized Q-meter output voltage from Eq. (3).

$$\frac{V_{out}(\xi)}{V_n} = \frac{Z_{eff}}{R_G} = \frac{1}{R_G} \frac{Z(\xi)}{1 + pZ(\xi)} = S_{eff}(\xi) + \iota T_{eff}(\xi) \tag{6}$$

can be considered an equivalent circuit impedance, Z_{eff}, of a two terminal, divided by the damping resistance R_G. In other words, using the general properties of two terminal relations [7], we can calculate the imaginary part of the Q-meter output voltage from the real part by using the Kramers — Kronig relation [7] for an impedance. Thus,

$$\frac{V_{out}(\omega)}{V_n} = S_{eff}(\omega) + \iota \frac{2\omega}{\pi} \mathcal{P} \int_0^\infty \frac{S_{eff}(\omega')\, d\omega'}{\omega'^2 - \omega^2}, \tag{7}$$

where $S_{eff} > 0$ for both signs of nuclear polarization and $\mathcal{P}$ means that the principal value of the integral be taken. In addition, the Kramers — Kronig relation can be formally applied to the difference of two impedances measured at $\xi \neq 0$ and $\xi = 0$ just as well as to Eq. (7). This difference

$$\frac{\Delta V_{out}(\omega)}{V_n} = \frac{V_{out}(\xi) - V_{out}(\xi = 0)}{V_n} = S(\omega) + \iota T(\omega) =$$

$$= S(\omega) + \iota \frac{2\omega}{\pi} \mathcal{P} \int_0^\infty \frac{S(\omega') d\omega'}{\omega'^2 - \omega^2}, \tag{8}$$

where

$$S(\omega) = S_{eff}(\xi) - S_{eff}(\xi = 0), \qquad S(\omega) < 0 \text{ or } S(\omega) > 0 \tag{9}$$

and

$$T(\omega) = T_{eff}(\xi) - T_{eff}(\xi = 0), \tag{10}$$

will be called the NMR signal because its real part, $S(\omega)$, and its imaginary part, $T(\omega)$, are nearly proportional to the imaginary (absorption) and real (dispersion) parts of the nuclear susceptibility, respectively. The real part of the NMR signal, $S(\omega)$, can be either positive or negative owing to the fact that it is the difference of two independent measurements. Using Eqs.(3,4,8) we get the NMR signal in terms of the circuit impedance Z

$$\frac{\Delta V_{out}(\omega)}{V_n} = \frac{1}{R_G} \frac{Z(\xi) - Z(\xi = 0)}{[1 + pZ(\xi)]\,[1 + pZ(\xi = 0)]}. \tag{11}$$

Then by defining a frequency-dependent complex function

$$G(\omega) = \rho^{-1}[1 + pZ_L(\xi = 0)][\rho + (r + \iota\omega L)\tanh(\gamma l)]\cosh(\gamma l) \tag{12}$$

we find the normalized NMR signal as

$$S(\omega) + iT(\omega) = \frac{\Delta V_{out}(\omega)}{V_n} = \frac{1}{R_G G(\omega)} \times$$

$$\times \frac{\iota\omega L\xi}{G(\omega) + \rho^{-1}\iota\omega L\xi\cosh(\gamma l)\{p\rho + [1 + p(R - \iota/\omega C_p)]\tanh(\gamma l)\}} \tag{13}$$

and thereby the equation for $\xi(\omega)$ in closed form is [6]

$$\xi(\omega) \equiv \eta\,\{\chi'(\omega) - \iota\chi''(\omega)\} = \frac{-\iota R_G G^2(\omega)}{\omega L} \times$$

$$\times \frac{\{\Delta V_{out}(\omega)/V_n\}}{1 - \rho^{-1}R_G G(\omega)\cosh(\gamma l)\{p\rho + [1 + p(R - \iota/\omega C_p)]\tanh(\gamma l)\}\{\Delta V_{out}(\omega)/V_n\}}, \tag{14}$$

where $\Delta V_{out}(\omega)/V_n$ (not to be confused with the modulation, M) is described by Eq.(8). According to Eq.(14), the actual NMR signals have to be transformed by a complex function to obtain the output signal as a linear function of nuclear susceptibility (see Fig.1).

It follows from the Kramers — Kronig relation for the susceptibility that the solution to Eq.(14) must satisfy the equation [8]

$$\xi'(\omega) - \xi'_{\infty} = \frac{2}{\pi} \mathcal{P} \int_0^{\infty} \frac{\omega' \xi''(\omega')\, d\omega'}{\omega'^2 - \omega^2} \tag{15}$$

which is the condition for self-consistency of the experimental data. If the signal wings are cut, then the imaginary part of the Q-meter signal cannot be accurately calculated by Eq.(8). Hence, an error is produced in the calculation of the susceptibility from Eq.(14), and in this case Eq.(15) will no longer be satisfied. We therefore propose that the real and imaginary parts of the Q-meter signal be measured, thus to avoiding any complications of using Eq.(8) in calculating $\xi'(\omega)$ via Eq.(14).

4. Discussion

Let us discuss the difference between the use of $S(\omega)$ and $\chi''(\omega)$ of Eq.(14) in determining the polarization from the integrated spectra. It has been shown [1,2,3] that the nuclear polarization is given approximately by

$$P \approx C \int_{\omega_{min}}^{\omega_{max}} S(\omega)\, d\omega, \tag{16}$$

where the integral is taken over the width $\omega_{max} - \omega_{min}$ of the frequency sweep. Comparing Eqs.(2,14,16) we come to the following conclusions:

1. The term $\xi(\omega)$ in the denominator of Eq.13 describes the experimentally observed difference in the form of the proton NMR line shape between opposite signs of polarization. We will calculate this distortion later in Section 4.2. The term $\Delta V_{out}(\omega)/V_n$ in the denominator of Eq.(14) allows one to find back $\chi(\omega)$ without distortions from the experimental signal.

2. Eq.(16) does not take into account the frequency dependence, causes a distortion for wide signals, most notably the false asymmetry of the deuteron signals. It can be shown, however, that the integral of a distorted signal $S(\omega)$ represents to a good approximation the polarization (Section 4.2).

3. Eq.(16) does not take into account the distortion of NMR signals due to phase errors. It causes, via $V_n(\omega)$ (see Eq.6), an additional mixing of $\xi'(\omega)$ and $\xi''(\omega)$ in Eq.(14), and thus this effect cannot be accounted for unless both the real and imaginary parts of the Q-meter output voltage are measured (Section 4.4).

4.1. The First Order Expansion

A first order solution can be found by a complex series expansion of Eqs.(3,4) about $\xi(\omega) = 0$. Alternatively, we find the first order approximation to $\xi(\omega)$ by setting $\Delta V_{out}(\omega)/V_n = 0$ in the denominator of Eq.(14) giving

$$\xi''(\omega) + \iota\xi'(\omega) = G^2(\omega)\left(\frac{R_G}{\omega L}\right)\left\{\frac{\Delta V_{out}(\omega)}{V_n}\right\}, \tag{17}$$

where $\Delta V_{out}(\omega)/V_n$ as

$$\xi'(\omega) = \frac{R_G}{\omega L}\{\mathrm{Im}\,(G^2)\,S(\omega) + \mathrm{Re}(G^2)\,T(\omega)\} \tag{18}$$

and

$$\xi''(\omega) = \frac{R_G}{\omega L}\{\mathrm{Re}\,(G^2)\,S(\omega) - \mathrm{Im}(G^2)\,T(\omega)\}. \tag{19}$$

If only the real part of the Q-meter signal is measured, then $T(\omega)$ is obtained from Eq.(8). Thus, in the linear approximation, the integral of the real part of the output voltage over the frequency sweep as in Eq.(16) is generally proportional to the nuclear polarization, since although according to Eqs.(18) and (19) $S(\omega)$ contains frequency dependent coefficients, these are independent of the polarization. However, the integral of $T(\omega)$ of Eq.(19) is non zero especially in the case of high polarized deuterons with asymmetric signals. For narrow symmetric signals, however, this proportionality is well obeyed even if the line shape $\xi''(\omega)$ changes as a function of the polarization.

4.2. The Line Shape Distortion of Proton Signals

We estimate the line shape distortion for protons from Eq.(14) with the values $\gamma l = 5\pi\iota$, $\tanh(\gamma l) = 0$, $G(\omega)\cosh(\gamma l) = 1$, $pR_G = 8.5$. The denominator of Eq.(14) becomes

$$1 - \rho^{-1}R_G G(\omega)\cosh(\gamma l)\left\{p\rho + \left[1 + p\left(R - \frac{\iota}{\omega C_p}\right)\right]\tanh(\gamma l)\right\}\left\{\frac{\Delta V_{out}(\omega)}{V_n(\omega)}\right\} \approx$$
$$\approx 1 - pR_G\left\{\frac{\Delta V_{out}(\omega)}{V_n}\right\} \approx 1 - 8.5\left\{\frac{\Delta V_{out}(\omega)}{V_n(\omega)}\right\}, \tag{20}$$

where $V_n = V_G A(\omega) \approx 5$ V. Consequently, the following equation, valid for the region near the Larmor frequency ($\xi' = 0$), is obtained for the output sig-

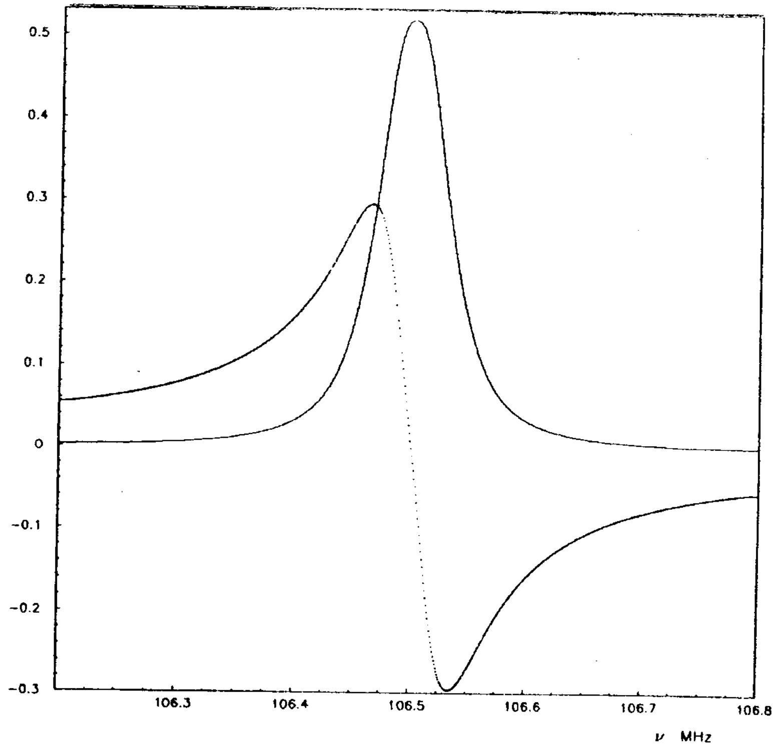

Fig.2. The dotted line shows the dispersion, $\xi'(\omega)$, and the solid line shows the absorption, $\xi''(\omega)$. These are the imaginary and real outputs of the Q-meter, respectively, after making a transformation by Eq.(14) using the proposed additions to the Q-meter shown in Fig.1. The line shape for the absorption signal is the modified lorentzian function $\xi''(\omega) \sim \sim \left[1 + \left|\frac{\omega - \omega_0}{\sigma}\right|^{2.54}\right]^{-1}$ found in [9]

nal for both positive and negative polarizations (sign of $\Delta V_{out}(\omega)$) for any frequency tuned cable ($\gamma l = 5\pi\iota$)

$$\xi''(\omega) = \frac{9.7\ \{\Delta V_{out}(\omega)/V_n(\omega)\}}{1 - 8.5\ \{\Delta V_{out}(\omega)/V_n(\omega)\}}. \tag{21}$$

Eqs.(20, 21) clearly show that the distortion as well as the nonlinearity of the output signal depend on the amplitude of the Q-meter output voltage and the shunting resistances R_i and R_G.

In order to better demonstrate the distortion of the proton signal shape we simulate the absorption part of the proton susceptibility by a Lorentzian-

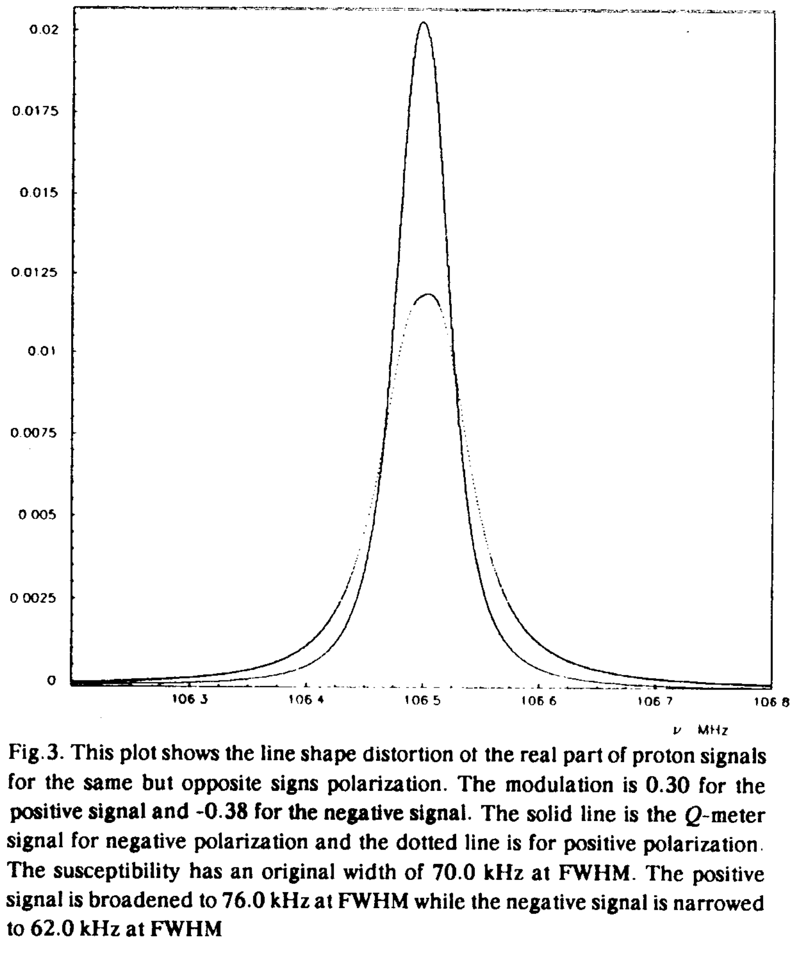

Fig.3. This plot shows the line shape distortion of the real part of proton signals for the same but opposite signs polarization. The modulation is 0.30 for the positive signal and -0.38 for the negative signal. The solid line is the Q-meter signal for negative polarization and the dotted line is for positive polarization. The susceptibility has an original width of 70.0 kHz at FWHM. The positive signal is broadened to 76.0 kHz at FWHM while the negative signal is narrowed to 62.0 kHz at FWHM

like function found in [9]. The dispersion is then calculated from Eq.(15) using the algorithm of Sperisen [10]; this is shown in Fig.2. The constant $\eta\chi_0$ is adjusted to give the desired value of the modulation (M). The simulation calculates the Q-meter output signal as a function of the susceptibility from Eqs.(3,4). The results are plotted in Figs.3,4. For the same but opposite sign of polarization, that is the same but opposite sign of susceptibility, we calculate the Q-meter output voltage and find that the positive polarization Q-meter signal ($M = 0.30$) is broadened to 76.0 kHz at FWHM whereas the negative polarization Q-meter signal (M=-0.38) is narrowed to 62.0 kHz at FWHM with respect to the width of the susceptibility of 70.0 kHz at FWHM. The proton signal amplitude is larger for negative polarization than

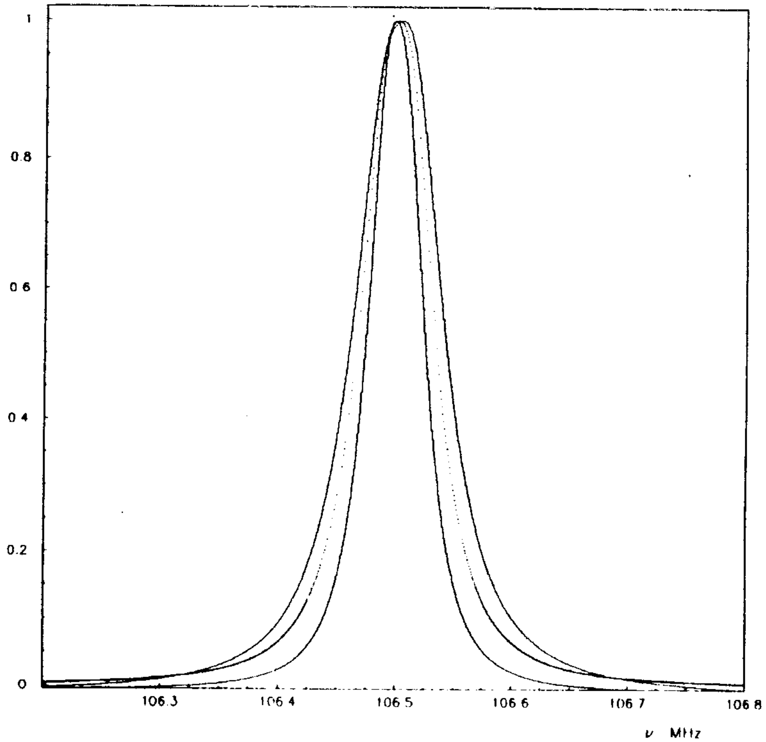

Fig.4. Same as Fig.3 except the Q-meter signals and absorptions have been normalized in order to highlight the line shape distortions. The widest line is the Q-meter signal for positive polarization, the narrowest line is the Q-meter signal for negative polarization and the middle (dotted) line is the susceptibility that generated the signals

for positive, as expected. The ratio of the area of the positive Q-meter output signal to the negative Q-meter output signal is 0.975.

4.3. The False Asymmetry of Deuteron TE Signals

The double peaks of the deuteron (spin $I = 1$) spectrum correspond to two quadrupole broadened transitions which partly overlap. If we define I_+ to be the intensity of $m = 1 \longleftrightarrow m = 0$ transition and I_- to be the intensity of $m = 0 \longleftrightarrow m = -1$ transition, where $m \equiv \langle I_z \rangle$, then the two deuteron peaks correspond to the I_+ and the I_- transitions. Defining the ratio of the intensities of these transitions as $R = I_+/I_-$ the deuteron polarization can be written in the well-known form

$$P_D = \frac{R^2 - 1}{R^2 + R + 1}. \tag{22}$$

Let us calculate the false asymmetry of the deuteron thermal equilibrium (TE) Q-meter calibration signal caused by the frequency dependent coefficient $G^2(\omega)/\omega$. According to the Maxwell — Boltzmann distribution, the natural polarization in 2.5 T field and at a temperature of T = 1 K, given by the Brillouin function (I = 1) as

$$P_D = \frac{4 \tanh(\hbar \omega_D / 2kT)}{3 + \tanh^2(\hbar \omega_D / 2kT)} = 0.00052, \tag{23}$$

where $\hbar$ is Plank's constant divided by 2π, k is Boltzmann's constant and $\omega_D = 2\pi \times 16.35$ MHz is the deuteron Larmor frequency for a magnetic field of 2.5 Tesla. For the TE polarization, the natural asymmetry of the deuteron signal is found from Eq.(22) as $R_{\text{nat}} = 1.00078$ when $P_D = 0.052\%$ from Eq.(23).

In order to estimate the false asymmetry we ignore the integral in Eq.(8) and assume that $r = \alpha = 0$, $r_{\text{eff}} \equiv |Z_L(\omega_0)| = R = 9\Omega$, $p = 0.02\Omega^{-1}$, $\omega L \approx \rho = 50\ \Omega$ so that we have from Eq.(17)

$$\xi''_{\pm 0} \equiv \xi''(\omega_{\pm 0}) \approx (1 + 2pr_{\text{eff}}) \left(1 - 2\pi \frac{\Delta\omega_{\pm 0}}{\omega_0}\right) \left(\frac{R_G}{\omega L}\right) \text{Re} \left(\frac{\Delta V_{\text{out}}(\omega)}{V_n}\right) \approx$$

$$\approx 20 \left(1 - 2\pi \frac{\Delta\omega_{\pm 0}}{\omega_0}\right) S_{\pm 0}, \tag{24}$$

where $\Delta\omega_0 = 0$ and $\Delta\omega_{\pm} \equiv \omega_{\pm} - \omega_0 = \pm 2\pi \times 60$ kHz is the half distance between the peaks of the NMR signal for deuterated 1-butanol d-10. Using an expression for the deuteron asymmetry from [11], we can compare the natural asymmetry to the experimentally measured asymmetry. The natural asymmetry $R_{\text{nat}} = 1.00078$ from Eqs.(22, 23), according to [11] must correspond to the peak susceptibility asymmetry

$$R_{\text{nat}} = \frac{\xi''_+ / \xi''_0 - 0{,}707}{\xi''_- / \xi''_0 - 0.707} = 1.00078. \tag{25}$$

To calculate the false asymmetry, we have to replace the values of susceptibility in Eq.(25) with the corresponding signal values, which should be calculated from Eq.(24). Thus,

$$R_{exp} = \frac{S_+/S_0 - 0{,}707}{S_-/S_0 - 0.707} = 1.075. \quad (26)$$

The signs (+, −, 0) in Eqs.(25, 26) are defined in [11] as the signal extrema for the respective I_+ and I_- transitions, and middle point of the deuteron signal respectively, and $S_{\pm 0}$ refers to the value of the real part of the signal at those points. From the deuteron experimental TE signals [12] we estimated the ratio $\xi''_+/\xi''_0 \approx \xi''_-/\xi''_0 = 1.95 \pm 0.05$ to calculate $S_\pm/S_0$ from Eq.(24) and R_{exp} using Eq.(26).

According to Eqs.(22, 26), the polarization is equal to 4.8% at $R_{exp} = 1.075$ due to the false asymmetry instead of 0.052% which is found by using the asymmetry value $R_{nat} = 1.00078$. The above example can be used to illustrate the difficulty in using Eq.(22) inversely to determine P_D from R_{exp}. We believe this effect explains the systematic difference between the values of polarization measured by the asymmetry method and the TE method. As a minimum requirement when analyzing enhanced deuteron signals, Eq.(24) must be used as a simple yet necessary correction to the false asymmetry.

4.4. The Distortions of NMR Signals Caused by Phase

Eq.(14) enables us to calculate the complex magnetic susceptibility from the NMR signal $S(\omega) + iT(\omega)$. However, the Q-meter output voltage, acting on the PSD input, incorporates the complex factor $V_n = A(\omega) V_G$ (see Eq.(8)).

$$\Delta V_{out} = A(\omega) V_G \{S(\omega) + iT(\omega)\}, \quad (27)$$

which must be taken into account for accurate measurements. We define the phase of the rf generator voltage to be zero. With this convention, the complex amplitude $A(\omega) V_G$ from Eq.(27) is

$$A(\omega) V_G = |A(\omega) V_G| \, e^{-i\Phi(\omega)}, \quad (28)$$

where $\Phi(\omega)$ is the phase shift of the amplifier, see Fig.1. The PSD output voltage is equal to

$$\Delta V_{PSD}(\omega) = |A(\omega) V_G| \, \{S(\omega) + iT(\omega)\} \, e^{-i[\Phi(\omega) - \phi(\omega)]}, \quad (29)$$

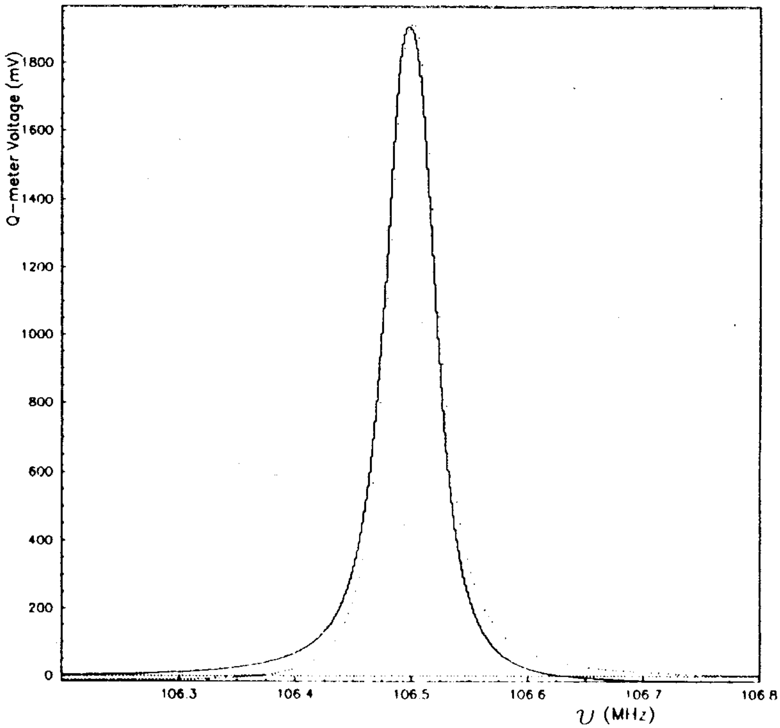

Fig.5. A plot of the distortion of proton signals due to phase shifts. For a symmetric absorption, the Q-meter output voltage is distorted when the phase Φ is non-zero. This plot corresponds to a constant phase of + 5.0° for the dotted line and a constant phase of − 5.0° for the solid line

where $\phi(\omega)$ is the phase of the voltage applied to the local oscillator (LO) input. We remind that the PSD output voltage does not depend on the amplitude of the LO voltage. It is usually assumed that the phase shift $\Phi(\omega)$ of the amplifier in the difference $\Phi(\omega) - \phi(\omega)$ is compensated approximately by using a similar amplifier at the reference input of the PSD (omitted in Fig.1). During the tuning procedure, in accord with Eq.(29) the phase difference $\Phi(\omega) - \phi(\omega)$ has to be accurately adjusted to zero at the frequency $\omega_0 = 2\pi\nu_0$, which is where $T(\xi = 0, \omega_0) = 0$ and $\mathrm{Im}\,\{Z\,(\xi = 0, \omega_0)\} = 0$ in Eq.(29). This is so that the PSD detects only the real part of the Q-meter output voltage

$$\mathrm{Re}\,(\Delta V_{\mathrm{PSD}}(\omega)) = |A(\omega) V_G|\; S(\omega), \tag{30}$$

which converted to zero intermediate frequency voltage in the PSD. In the absence of the imaginary part of this voltage, the phase tuning of the Q-meter may be done only approximately using the characteristic Q-curve shape. The error in the setting of the phase relation of PSD gives rise to additional distortion of the signal. It is evident from the plots in Fig.5 showing the proton signal for the phase errors of + 5 and − 5 degrees. Comparing with plots of Fig.4, which were calculated with $\phi = 0$, we see the substantial distortion, predominantly in the antisymmetric features appearing in the signal wings. Due to this the integral in Eq.(2) may deviate form the original value by an amount which depends strongly on the zero line position (see Section 6). The Q-meter with detection of the real and imaginary parts will allow more accurate phase tuning in additional to the extraction of the true susceptibitliy, using Eq.(14), including the phase correction function $\Phi(\omega) - \phi(\omega)$ in Eq.(29).

5. The Shape of the Q-curve

An accurate TE-calibration normally requires a special experimental procedure (such as immersion in superfluid helium-4) to maintain the sample material at a homogeneous and accurately known temperature where the polarization is described by the Brillouin function. This calibration then remains valid for some period of time during which the polarization is determined by comparison of the integrated signals to the TE signals. After the calibration, we have to estimate and correct in some way the influence of circuit parameter drift on the measurement of target polarization.

Another problem arises with the TE-calibration of small signals such as those of the deuteron. Circuit parameter drift leaves a residual Q-curve, the differential Q-curve (due to temperature drift) superimposing with the TE signal, whose integral can be greater than that of the TE signal. In this case, the TE-calibration is dependent on the procedure used to subtract the Q-curve. Consequently, we would like to know the true equation for the residual Q-curve.

Both problems are addressed by fitting Eqs.(3,4) with $\xi = 0$ to the measured Q-curves, thus determining the circuit parameters and the residual Q-curve.

The Q-curve is calculated from the real part of Eq.(3) with $\xi = 0$. Separating the real and imaginary parts of Eq.(3) gives [3]

$$\mathrm{Re}\left\{\frac{V_{\mathrm{out}}(\omega)}{V_n}\right\} = \frac{1}{R_G}\left\{\frac{\mathrm{Re}\,(Z) + p\{\mathrm{Re}^2(Z) + \mathrm{Im}^2(Z)\}}{[1 + p\,\mathrm{Re}(Z)\,]^2 + p^2\mathrm{Im}^2(Z)}\right\} \tag{31}$$

and

$$\mathrm{Im}\left\{\frac{V_{\mathrm{out}}(\omega)}{V_n}\right\} = \frac{1}{R_G}\left\{\frac{\mathrm{Im}(Z)}{[1 + p\,\mathrm{Re}(Z)\,]^2 + p^2\mathrm{Im}^2(Z)}\right\}. \tag{32}$$

The real part can be rewritten in the form

$$\mathrm{Re}\left\{\frac{V_{\mathrm{out}}(\omega)}{V_n}\right\} = \frac{1}{pR_G}\left\{1 - \frac{1 + p\,\mathrm{Re}(Z)}{[1 + p\,\mathrm{Re}(Z)\,]^2 + p^2\mathrm{Im}^2(Z)}\right\} \tag{33}$$

Then using relations taken from [1] and applying them to Eq.(4) we find [6]

$$\mathrm{Re}\left\{\frac{V_{\mathrm{out}}(\omega)}{V_n}\right\} =$$

$$= \frac{1}{pR_G}\left\{1 - \frac{1 + p(R + A_1/A_0)}{[1 + p(R + A_1/A_0)\,]^2 + p^2[A_2/A_0 - 1/\omega C_p]^2}\right\}, \tag{34}$$

where

$$A_0 = 1 - 2k_2\frac{\omega L}{\rho} + 2k_1\frac{r}{\rho} + (k_1^2 + k_2^2)\left\{\left(\frac{r}{\rho}\right)^2 + \left(\frac{\omega L}{\rho}\right)^2\right\}, \tag{35}$$

$$A_1 = r\left\{1 + k_1\frac{r}{\rho} + (k_1^2 + k_2^2)\right\} + \rho k_1\left\{1 + \left(\frac{\omega L}{\rho}\right)^2\right\} \tag{36}$$

and

$$A_2 = \omega L\,\{1 - (k_1^2 + k_2^2)\} + \rho k_2\left\{1 - \left(\frac{r}{\rho}\right)^2 - \left(\frac{\omega L}{\rho}\right)^2\right\}. \tag{37}$$

We have made use of the relation $\tanh(\gamma l) = k_1 + \iota k_2$, where

$$k_1 = \frac{\tanh(\alpha l)}{k_3\cos^2(\beta l)},\quad k_2 = \frac{\tan(\beta l)}{k_3\cosh^2(\alpha l)},\quad k_3 = 1 + \tanh^2(\alpha l)\tan^2(\beta l). \tag{38}$$

It is clear from Eq.(34) that the resonance value for the capacitance is very close to $C_p = A_0/A_2/\omega$ so this formula can be used for either a hybrid or normal resonance circuit.

Using this method, a baseline fit can be made at any time in order to calculate new values for the drifting circuit parameters. These new values can then be used in Eq.(14) to correct the NMR signals, thus producing a method to compensate for parameter drift in the time between measuring the TE-calibration signals.

Let us determine as an example the drift in the baseline during the TE-calibration due to the temperature drift of γl, we take the derivative with respect to γl of Eq.(3) at $\xi = 0$ which gives

$$\frac{V_{out}(\iota\gamma(t)) - V_{out}(\iota\gamma(t=0))}{V_n} = \left\{\frac{\rho^2 - (r + \iota\omega L)^2}{\rho R_G G^2(\omega)}\right\}\{\iota\gamma(t) - \iota\gamma(t=0)\}, \quad (39)$$

where $\gamma(t = 0)$ is the value of the complex propagation constant at the start of the TE-calibration and $\gamma(t)$ is its value a time t later. These values are determined by fitting Eq.(34) to the baseline signal.

6. Errors in the Polarization Calculation

Within the scope of the series Q-meter, it is useful to mention some important considerations in the calculation of the polarization. As is well known, the absorption part of the susceptibility describes the frequency distribution of the spins near the NMR Larmor frequency, and its integral is proportional to the nuclear polarization. Strictly speaking, the polarization is

$$P = C\int_0^{\infty} \xi'(\omega)\, d\omega. \quad (40)$$

However, in practice the absorption can only be measured in a small range around the Larmor frequency. Thus, the integral in Eq.(40) is measured over restricted limits. Moreover, it is generally assumed that the Q-meter signal, $S(\omega)$, is proportional to $\xi''(\omega)$ and that

$$P = C_s\int_0^{\infty} S(\omega)\, d\omega, \quad (41)$$

where the constant of proportionality, C_s is a function of the modulation, the circuit parameters, and the target material. But, the general theory of linear two terminals [7] tells us that the integral in Eq.(41) can be calculated independent of the circuit parameters as

$$\int_0^{\infty} \{S(\omega) - S_{\infty}\}\, d\omega = -\frac{\pi}{2}\lim_{\omega\to\infty} \omega T(\omega), \quad (42)$$

where $S(\omega)$ and $T(\omega)$ were described in Eq.(8) and

$$S_{\infty} = \lim_{\omega\to\infty} S(\omega). \quad (43)$$

Typically the wings of an absorption line fall down faster than for a Lorentzian function. For a Lorentzian shape, the absorption and dispersion will fall off asymptotically at least as fast ω^{-2} and ω^{-1} respectively. Multiplying

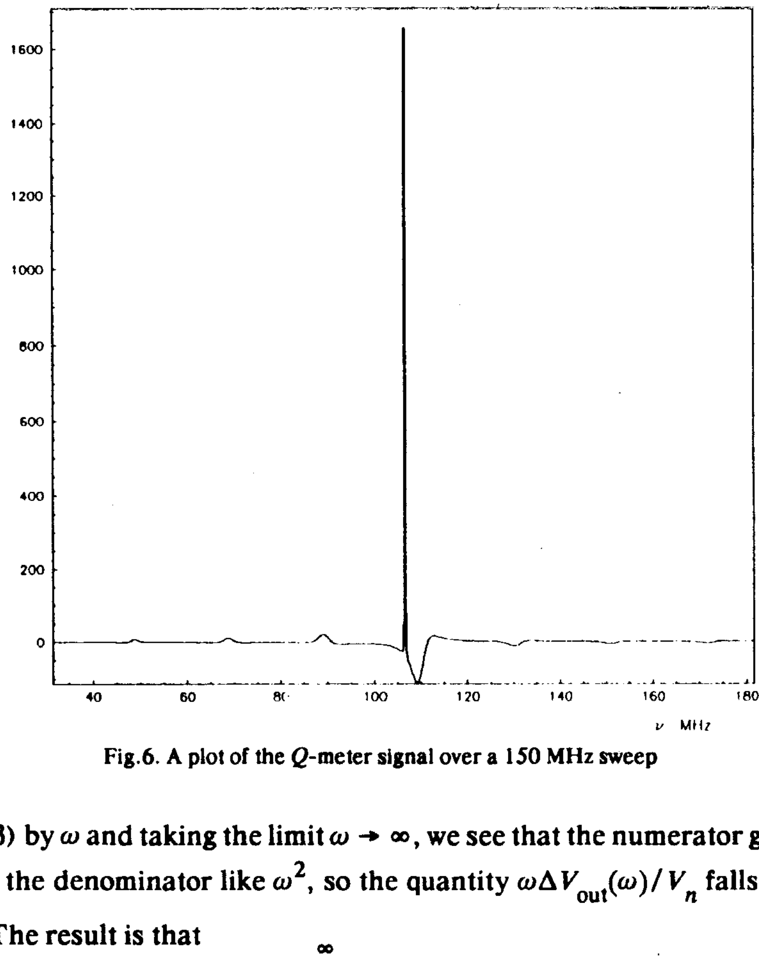

Fig.6. A plot of the Q-meter signal over a 150 MHz sweep

Eq.(13) by ω and taking the limit $\omega \rightarrow \infty$, we see that the numerator goes like ω and the denominator like ω^2, so the quantity $\omega \Delta V_{out}(\omega)/V_n$ falls off like ω^{-1}. The result is that

$$\int_0^\infty S(\omega) = 0 \tag{44}$$

such that the integral is not dependent on the receiving circuit's parameters. The function $S(\omega)$ is plotted in Fig.6 for a very wide sweep. The effect of the cable and slowly decaying dispersion tail on the circuit inductance is visible. In this figure, the cable nodes occur every 21.3 MHz, which is what is expected for a cable with length $5\lambda/2$ at 106.5 MHz Larmor frequency.

The shape of the signal must be taken into account when designing the Q-meter and when calculating the errors in the polarization measurement. In fact, one can see from Figs.3 and 5 that signal crosses the zero line on both sides of the Larmor frequency. This produces an extra error depending on where one draws the line about which $S(\omega)$ is integrated. That is, the signal voltage should be allowed to cross zero when calculating the integral,

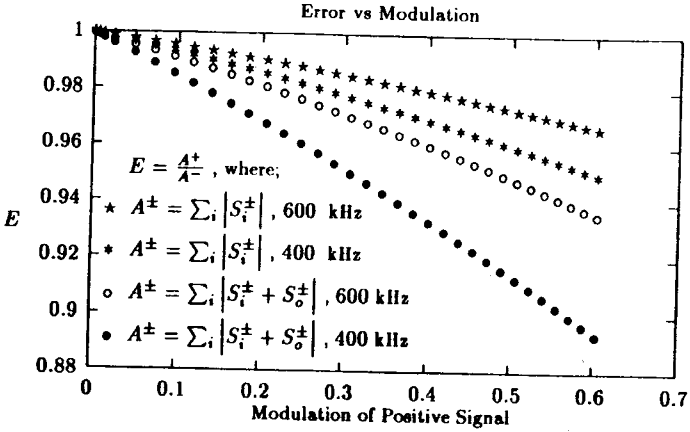

Fig.7. An illustration of error in the proton polarization measurement shown as a function of modulation M for positive polarization. The measure of error is the ratio of the positive signal's integral to the negative signal's integral for susceptibilities differing only in sign. The constant $S_0(\omega)$ is an offset added so that each signal has the same sign over the entire frequency sweep (i.e., the signal wings do not cross zero)

and should not be offset such that it always has the same sign. There is a difference of a factor of two in the error for the two cases. This is plotted in Fig.7.

7. Conclusions

We have presented a new Q-meter theory for accurate measurements of nuclear polarization. From this analysis it is clear that new techniques must be developed based on the principles embodied in Eqs.(14,34) of this paper because the usual methods, based on series expansions of Eqs.(3,4), cannot be easily adapted to correct experimental data. We list the next steps in the development of polarization measurements:

1. The series Q-meter [5] needs to be improved by the addition of a separate phase sensitive detector to measure the imaginary part as well as the real part of the Q-meter output signal. Also, one ought to add a function converter (see Fig.1) which calculates $\xi(\omega)$ from $\Delta V_{out}(\omega)$ via Eq.(14). It is $\xi(\omega)$, not $\Delta V_{out}(\omega)$, whose integral is exactly proportional to the nuclear polarization. The reason for measuring the imaginary part of the Q-meter signal is to avoid the numerical calculation of the integral in Eq.(8), thus allowing fast and accurate corrections due to dispersion effects.

2. The origins of the false asymmetry of the deuteron signal and the distortions of the proton signal are demonstrated and henceforth can be accounted for.

3. It is proposed to determine circuit parameters by fitting Eq.(34) to data. This would allow a method for accurate correction of the polarization for circuit parameter drift during long periods between TE calibrations.

4. The experimental calibration signals can be corrected for the residual Q-curve by fitting Eq.(39) to real data. This residual contribution is caused by temperature drift of circuit elements such as the complex propagation constant γ during long time it takes to gain high statistics for the TE-signals.

5. The susceptibility now be corrected for errors caused by the dependence of the phase on the frequency. Within the scope of this theory, the effects of phase distortions can now be accounted for for the first time.

Acknowledgements

This work has been made within the Spin Muon Collaboration (SMC) at CERN. We would like to thank C.Whitten, F.Lehar and D.Pose for useful remarks. Y.K. is grateful to V.Hughes, G.Mallot, R.Voss for support. This work was partially supported by the US Department of Energy, the Laboratory of Particle Physics (JINR) and the SMC.

We wish to thank Yannis Semertzidis for helpful discussions, many of which led to corrections in the numerical calculations performed in this work.

References

1. Petricek V. — Nucl. Instr. and Meth., 1968, 58, p.111.
2. Ryter C. — Nucl. Instr. and Meth., 1967, 49, p.267.
3. Niinikoski T.O. — In: Proc. of the 2nd Int. Workshop on Polarized Target Materials, G.R.Court, D.A.Cragg and T.O.Niinikoski (eds.), report RL-80-080, SRC,Rutherford Laboratory, 1980, p.80.
4. Gifford D. — In: Proc. of the 2nd Int. Workshop on Polarized Target Materials, G.R.Court, D.A.Cragg and T.O.Niinikoski (eds.), report RL-80-080, SRC, Rutherford Laboratory, 1980, p.85.
5. Court G.R., Gifford D.W., Harrison P., Heyes W.G., Houlden M.A. — Nucl. Instr. and Meth., 1993, A324, p.433.
6. Kisselev Yu.F. — The Theory of Q-Meter, Geneva, CERN, SMC note, 1993, 20.
7. Bode Hendrik W. — Network Analysis and Feedback Amplifier Design, New York: Van Nostvard, 1945 (repr. 1953), p.563.

8. Abragam A. — The Principles of Nuclear Magnetism, Clarendon Press, Oxford, p.93.
9. Hill John J., Hill Daniel A. — Nucl. Instr. and Meth., 1974, 116, p.269.
10. Sperisen F. — Nucl. Instr. and Meth., 1987, A260, p.455.
11. Kisselev Yu.F., Popov S.A., Fedorov A.N. — Pis'ma Zh. Eksp. Teor. Fiz., January 25, 1992, 55, No.2, p.99.
12. Magnon A. and Polarized Target Group, CERN (PPE) — Saclay, SMC note, 1992, 15, p.24.

Received on March 3, 1994.